

The Slow Folding Reaction of Barstar: the Core Tryptophan Region Attains Tight Packing Before Substantial Secondary and Tertiary Structure Formation and Final Compaction of the Polypeptide Chain

K. Sridevi^{1,2}, Juhi Juneja¹, Abani K. Bhuyan^{1,3}, G. Krishnamoorthy^{2*} and Jayant B. Udgaonkar^{1*}

¹National Centre for Biological Sciences, Tata Institute of Fundamental Research, GKVK Campus, Bangalore 560 065 India

²Department of Chemical Sciences, Tata Institute of Fundamental Research, Homi Bhabha Road, Mumbai 400 005 India

³Jawaharlal Nehru Centre for Advanced Scientific Research Jakkur, Bangalore 560064, India

The slow folding of a single tryptophan-containing mutant of barstar has been studied in the presence of 2 M urea at 10 °C, using steady state and time-resolved fluorescence methods and far and near-UV CD measurements. The protein folds in two major phases: a fast phase, which is lost in the dead time of measurement during which the polypeptide collapses to a compact form, is followed by a slow observable phase. During the fast phase, the rotational correlation time of Trp53 increases from 2.2 ns to 7.2 ns, and its mean fluorescence lifetime increases from 2.3 ns to 3.4 ns. The fractional changes in steady-state fluorescence, far-UV CD, and near-UV CD signals, which are associated with the fast phase are, respectively, 36 %, 46 %, and 16 %. The product of the fast phase can bind the hydrophobic dye ANS. These observations together suggest that the folding intermediate accumulated at the end of the fast phase has: (a) about 20 % of the native-state secondary structure, (b) marginally formed or disordered tertiary structure, (c) a water-intruded and mobile protein interior; and (d) solvent-accessible patches of hydrophobic groups. Measurements of the anisotropy decay of Trp53 suggest that it undergoes two types of rotational motion in the intermediate: (i) fast ($\tau_r \approx 1$ ns) local motion of its indole side-chain, and (ii) a slower ($\tau_r \approx 7.2$ ns) motion corresponding to global tumbling of the entire protein molecule. The ability of the Trp53 side-chain to undergo fast local motion in the intermediate, but not in the fully folded protein where it is completely buried in the hydrophobic core, suggests that the core of the intermediate is still poorly packed. The global tumbling time of the fully folded protein is faster at 5.6 ns, suggesting that the volume of the intermediate is 25 % more than that of the fully folded protein. The rate of folding of this intermediate to the native state, measured by steady-state fluorescence, far-UV CD, and near-UV CD, is $0.07(\pm 0.01) \text{ min}^{-1}$. This rate compares to a rate of folding of $0.03(\pm 0.005) \text{ min}^{-1}$, determined by double-jump experiments which monitor directly formation of native protein; and to a rate of folding of 0.05 min^{-1} , when determined from time-resolved anisotropy measurements of the long rotational correlation time, which relaxes from an initial value of 7.2 ns to a final value of 5.6 ns as the protein folds. On the other hand, the amplitude of the short correlation time decreases rapidly with a rate of $0.24(\pm 0.06) \text{ min}^{-1}$. These results suggest that tight packing of residues in the hydrophobic core occurs relatively early during the observable slow folding reaction, before substantial secondary and tertiary structure formation and before final compaction of the protein.

© 2000 Academic Press

Keywords: barstar; core packing; time-resolved fluorescence; rotational correlation time; protein folding

*Corresponding author

Abbreviations used: CD, circular dichroism, ANS, 8-anilinonaphthalene sulfonate.
E-mail address of the corresponding author: jayant@ncbs.res.in

Introduction

It is generally accepted that on being driven to folding conditions, unfolded polypeptides contract and collapse. Considerable uncertainty exists regarding the nature, specificity, and productivity of the collapse reaction (Dill *et al.*, 1995; Gutin *et al.*, 1995; Nymeyer *et al.*, 1998; Sali *et al.*, 1994; Thirumalai, 1995). Reports on the non-specific nature of polypeptide collapse have appeared (Agashe *et al.*, 1995; Chan *et al.*, 1997; Sosnick *et al.*, 1997), and counter-arguments have also been presented that collapsed products represent early intermediates that guide the folding protein to arrive at its native state (Roder & Colon, 1997; Shastry & Roder, 1998). The obvious approach to understand the nature and specificity of chain collapse and condensation is to analyze the structure as well as the local and global dynamics of the condensed product, and to study how the structure and dynamics evolve as the folding reaction progresses.

For some time now, it has been possible to monitor, with millisecond time resolution, secondary structure formation during folding, using the methods of stopped-flow circular dichroism (Kuwajima *et al.*, 1987) or pulse-labeling by hydrogen exchange (Roder *et al.*, 1988; Udgaonkar & Baldwin, 1988). More recently, direct fast measurements of collapse during folding have become possible using methods exploiting small angle X-ray scattering (Eliezer *et al.*, 1995; Chen *et al.*, 1998; Segel *et al.*, 1999; Semisotnov *et al.*, 1996), dynamic light scattering (Gast *et al.*, 1998), dilatometry (Ybe & Kahn, 1994), and time-resolved fluorescence spectroscopy (Jones *et al.*, 1995; Beechem, 1997; Bilsel *et al.*, 1999). For proteins that appear to fold without apparent accumulation of any folding intermediate, it appears that diffusive collapse occurs concomitantly with the rate-limiting step in folding (Jacob *et al.*, 1997; Ladurner & Fersht, 1999; Panick *et al.*, 1998; Plaxco & Baker, 1998; Plaxco *et al.*, 1999), which suggests that collapse and formation of specific structure are coupled. For other proteins, collapse occurs rapidly in a step that is not rate limiting, and leads either to the formation of compact pre-molten globule forms in which secondary structure is absent (Agashe *et al.*, 1995) or very unstable, or to the direct formation of compact molten globule forms with partial but more stable native-like secondary structure (Ptitsyn, 1992).

Little is, however, known about the coupling of the initial events of folding, chain collapse and secondary structure formation, to later events such as the formation of specific tertiary interactions (Waldburger *et al.*, 1996) or tight packing of the protein (Munson *et al.*, 1997), both of which might be rate-limiting steps during folding. Methods for studying these later events have usually been indirect, and include the elegant protein engineering approach (Matouschek *et al.*, 1990). A study of the role of packing interactions during the folding

process is especially important because they play an important role in determining the stability and structure of the fully folded protein (Alber & Matthews, 1987; Axe *et al.*, 1996; Bashford *et al.*, 1987; Daopin *et al.*, 1991; Gassner *et al.*, 1996; Lim & Sauer, 1989, 1991; Munson & Regan, 1996; Reidhaar-Olson & Sauer, 1988).

The folding pathway of barstar, an 89-residue protein inhibitor of the ribonuclease barnase, has been studied extensively (Agashe *et al.*, 1995; Bhuyan & Udgaonkar, 1999; Nolting *et al.*, 1995, 1997; Schreiber & Fersht, 1993; Shastry *et al.*, 1994; Shastry & Udgaonkar, 1995). Both fast and slow-folding reactions are seen; these originate from two unfolded forms of the protein that differ in isomerization of the Tyr47-Pro48 bond (Schreiber & Fersht, 1993; Shastry *et al.*, 1994). A fast collapse occurs in the sub-millisecond time domain (Agashe *et al.*, 1995; Nolting *et al.*, 1995, 1997). Subsequent structure formation in the next 50-200 ms leads to the formation of the intermediate, I_N , that has been reported to be sufficiently folded to be active (Schreiber & Fersht, 1993). Nevertheless, I_N is still considerably molten globule like: it has exposed hydrophobic patches, which enable it to bind ANS (Shastry & Udgaonkar, 1995), it has only partial secondary structure and very little specific tertiary structure (Bhuyan & Udgaonkar, 1999). So far, there has been no information available on the degree of compactness or packing or on the consolidation of the core in I_N .

In this article we report on the structural and dynamic properties of I_N , monitored by the use of steady-state and time-resolved tryptophan fluorescence, and far-UV and near-UV CD. A mutant form of barstar, W38FW44F, which contains only a single tryptophan, Trp53, buried in the protein interior, was used for the study. Earlier studies had shown that the stability and folding of W38FW44F are similar to those of the wt protein (Nath *et al.*, 1996; Swaminathan *et al.*, 1996). Time-resolved measurements of the decay of fluorescence anisotropy of Trp53 in I_N show that the decay has at least two components: a 1 ns component representing local motion of the Trp53 side-chain, and a 7.2 ns component representing the global tumbling motion of the protein molecule. In contrast, the decay of fluorescence anisotropy in N has only a single 5.6 ns component representing the global tumbling motion. The larger magnitude of the longer decay component in I_N indicates that it has a hydrodynamic volume larger than that of the native state, and the presence of the 1 ns component in I_N but not in N indicates that the former, unlike the latter, does not possess a well-packed protein core. I_N folds to the native state in two slow steps. In the faster of the two steps, the protein core becomes progressively rigid as seen by the decreasing mobility of the tryptophan side-chain, accompanied by disappearance of the 1 ns component in the decay of anisotropy. In the slower step, the folding chain acquires more than

half of the native state secondary structure (as measured by far-UV ellipticity) and nearly two-thirds of the specific tertiary structure (as measured by near-UV ellipticity), and acquires concomitantly the dimensions of the fully folded protein.

Results

Equilibrium-unfolding measurements

The urea-induced equilibrium unfolding transition of W38FW44F at 10 °C was monitored using the fluorescence intensity of Trp53 at 330 nm as the probe. Figure 1 shows the fraction of native

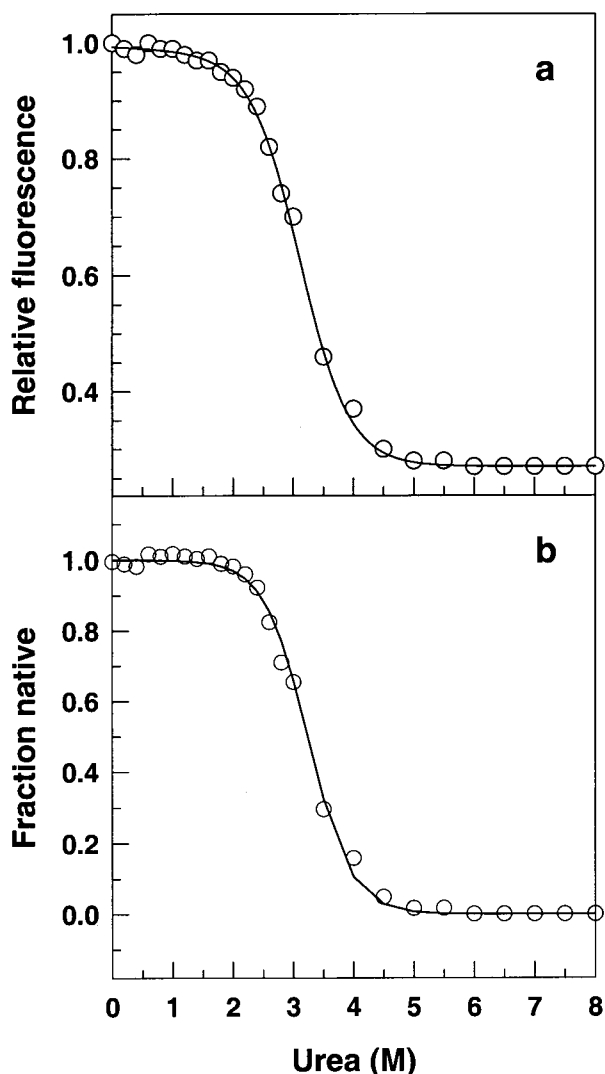


Figure 1. Equilibrium unfolding curve of W38FW44F at 10 °C monitored by steady-state fluorescence (a). The fraction of native protein calculated (equation (5a)) from the fluorescence intensity at 330 nm at different urea concentrations (b). The continuous line through the data is a non-linear least-squares fit of the data to equation (5b). The concentration of the protein used was 5 μ M in 20 mM phosphate, 0.3 mM EDTA, 0.25 mM DTT at pH 7. The excitation was at 295 nm.

molecules at different urea concentrations as calculated from the raw data using equation (5a). The continuous line through the data is the fit according to equation (5b). The ΔG and C_m values for the melting transition, which starts at 2 M urea, are 4.7(\pm 0.4) kcal mol⁻¹ and 3.2(\pm 0.2) M, respectively. The value of 1.76 kcal/mol for ΔG in 2 M urea, 10 °C, indicates that <5% of the protein molecules are unfolded in these conditions. The steady state and time-resolved fluorescence properties of the protein in the presence of 2 M urea are identical to those in the absence of any denaturant (see below). Kinetic experiments on refolding were done by diluting the protein from 8 M urea into a final denaturant concentration of 2 M.

Formation of native protein during folding

The relative amount of native protein was determined at each time of folding in 2 M urea, 10 °C, by double-jump experiments, in which the amount of N was determined by an unfolding assay (Schreiber & Fersht, 1993; Shastry *et al.*, 1994; Shastry & Udgaonkar, 1995). It is seen that at the earliest time of measurement (30 seconds) itself, 33(\pm 4)% of the protein molecules have already folded to N (Figure 2). The remaining 67% of the molecules fold to N in the observable time window. Given the errors in the determination of N at each time point, the kinetics of folding can be

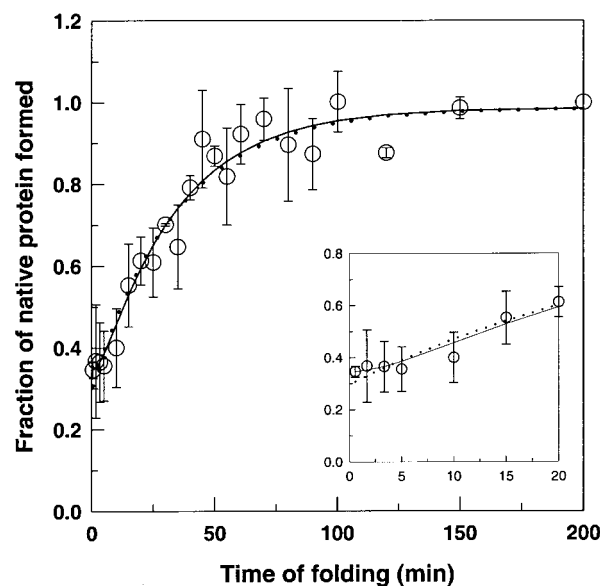


Figure 2. Kinetics of formation of native protein during folding in 2 M urea, pH 7, 10 °C. The relative amount of native protein at different times of folding was determined by means of double-jump experiments, in which native protein was identified by an unfolding assay (see Materials and Methods). The continuous line through the data is a non-linear least-squares fit of the data to equation (4) (with $S_{IN'} = 0$, $k_1 = 0.24$ min⁻¹). The error bars represent the spread in the values obtained from two separate experiments. A value of 0.03(\pm 0.005) min⁻¹ was obtained for k_2 . The dotted line represents a single exponential fit through the data.

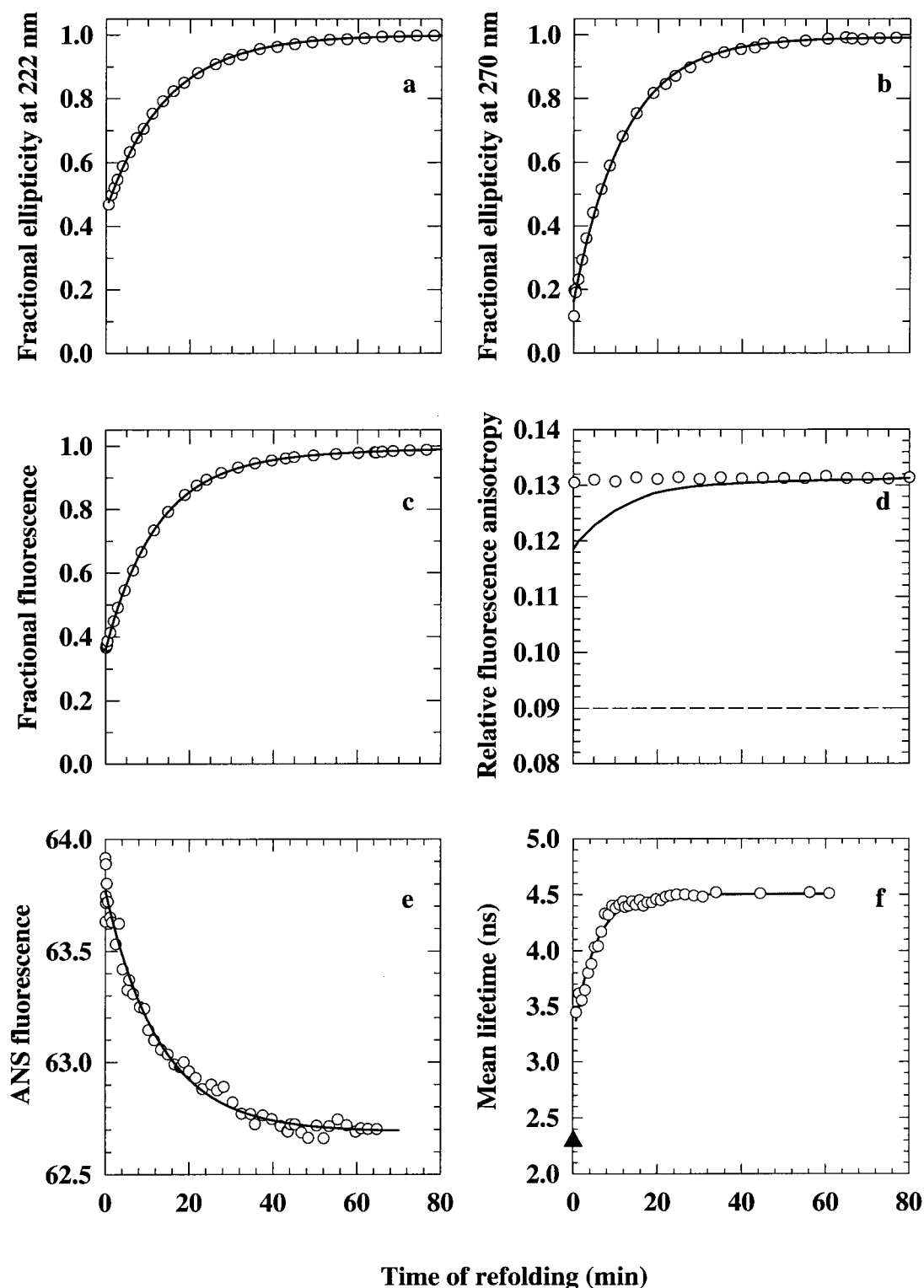


Figure 3. Kinetics of folding of W38FW44F at 10°C monitored by measurement of far-UV CD at 222 nm (a), near-UV CD at 270 nm (b), intrinsic tryptophan fluorescence intensity at 330 nm (c), steady state intrinsic tryptophan fluorescence anisotropy at 330 nm (d), ANS fluorescence at 480 nm upon excitation at 380 nm (e) and mean tryptophan fluorescence lifetime of Trp53 (f). Folding was initiated by diluting urea from 8 M to 2 M. In (a), (b) and (c), the data have been normalized such that the total amplitude of change in the optical property from the unfolded to the native state is 1. The continuous line in (d) was simulated using the fluorescence intensity data (c) and the two-state model (see the text), and the broken line represents the fluorescence anisotropy of the protein in 8 M urea. In (e) folding was initiated by diluting urea from 8 M to 2 M into a buffer containing 100 μ M ANS. Final protein concentration was \sim 5 μ M. In (f) the filled triangle at zero time corresponds to the value for protein in 8 M urea (before dilution to 2 M urea). Continuous lines through the experimental points in (a), (b), (c), and (e) are fits to equation (4) using a value for k_1 of 0.24 min^{-1} which was obtained as the rate of change in amplitude of the faster rotational correlation

described equally well either by equation (4) (see Discussion) or by single exponential kinetics. Either fit yields an apparent rate of formation of N of $0.03(\pm 0.005) \text{ min}^{-1}$.

CD and fluorescence-monitored folding

Kinetics of folding initiated manually by transferring the unfolded protein from 8 M urea to a final concentration of 2 M, probed by far-UV CD at 222 nm, near-UV CD at 270 nm, fluorescence intensity at 330 nm (I_{SS}), and steady-state fluorescence anisotropy (r_{SS}), are shown in Figure 3(a)-(d). In all of these experiments, a fraction of the total expected amplitude, i.e. the difference in signal intensity between the fully folded and the fully unfolded protein, is lost within the dead time of measurements. This observation, given a dead time of several seconds, is not surprising. It is, however, interesting that the amplitude of the burst phase signal, S_0^{fol} , differs strikingly from one probe of measurement to the other. Thus, S_0^{fol} values measured by steady-state fluorescence, far-UV CD, near-UV CD, and fluorescence anisotropy account for, respectively, 36%, 46%, 16%, and almost 100% of the total amplitude. The time-dependent changes in signal of each of the three optical probes accompanying folding were fitted according to equation (4) (Figure 3(a)-(c)). The rates of slow folding measured by the I_{SS} and the far and near-UV CD data are similar ($0.07(\pm 0.01) \text{ min}^{-1}$).

Kinetic curves using far-UV CD as the measuring probe were determined not only at 222 nm, but also at seven other wavelengths between 216 and 230 nm (data not shown). The fractional change in the amplitude of the reaction, which was lost in the dead time of measurement was independent of wavelength, with a value of $0.46(\pm 0.02)$. The apparent rate of the observable phase was also independent of wavelength with a value of $0.07(\pm 0.01) \text{ min}^{-1}$.

The results obtained by steady-state measurement of circular dichroism and fluorescence intensity therefore indicate that the protein folds in two phases: a fast phase lost as the burst kinetics, and an observable slow phase arising from the time evolution of the product of the fast phase. As the time evolution of steady-state anisotropy shows (Figure 3(d)), the overall rotational dynamical properties of the product(s) of the fast phase of folding are very similar to those of the native protein. The continuous line in this panel describes the time dependence of changes of r_{SS} calculated by assuming a two-state model (equations (6)-(9)). To summarize these results, the slow phase of folding

of barstar involves the transition of an intermediate to the native state. The intermediate and the native state are structurally quite different, even though the two forms appear to have similar tumbling times in the solution.

To obtain qualitative information about the existence of exposed hydrophobic patches on the intermediate, the kinetics of refolding were measured by allowing the protein to refold in the presence of ANS (8-anilino-1-naphthalene sulfonate). This hydrophobic molecule binds to clusters of apolar groups in proteins when they are hydrated (Stryer, 1965). Previous work on the refolding of barstar also describes the use of ANS (Shastry *et al.*, 1994), and the binding of ANS to I_N is best described by a 1:1 stoichiometry and a dissociation constant of $125 \mu\text{M}$ (Shastry & Udgaonkar, 1995). In the present study, refolding was initiated by transferring one part of the unfolded protein from 8 M urea to three parts of the aqueous refolding medium containing $\sim 100 \mu\text{M}$ ANS at 10°C . If the folding intermediate contains solvent-exposed apolar clusters, ANS will bind to these sites. The folding of the intermediate to the native state is accompanied by dissociation of ANS, which can be monitored by measuring its fluorescence. The time course of decrease of ANS fluorescence during refolding is shown in Figure 3(e). Fitting the data, to equation (4) yields a rate of 0.08 min^{-1} , comparable with the folding rate ($0.07(\pm 0.01) \text{ min}^{-1}$) measured by the other steady-state probes (Figure 3(a)-(c)).

Figure 4 compares the fluorescence spectrum acquired within 45 seconds of initiation of refolding in 2 M urea to the fluorescence spectra of fully folded and fully unfolded (in 8 M urea) proteins. The spectrum at 45 seconds is broad compared to both the fully folded and unfolded protein spectra, in part because it has a contribution from 33% of the molecules which have already folded to the native state, and it is blue shifted with respect to the unfolded protein spectrum, and red shifted with respect to the fully folded spectrum. These results suggest that the Trp53 in the core of the intermediate formed in the first minute of folding is still hydrated, although to a lesser extent than in the unfolded protein. The quantum yield of the Trp53 fluorescence in the intermediate is also seen to be substantially lower than that in the fully folded protein, again indicative of the intermediate possessing a solvent-accessible core. In summary, the steady-state spectroscopic data in Figures 3 and 4 indicate that an intermediate with partial secondary structure, exposed hydrophobic patches, and very little tertiary structure is formed within the first minute of refolding.

time τ_{r2} , which is described by equation (3) (Figure 6(b)). The continuous line through the data in (f) is also a single exponential fit and yields a rate constant of 0.16 min^{-1} . Values obtained for k_2 were 0.07 min^{-1} (a), 0.08 min^{-1} (b) 0.08 min^{-1} (c), and 0.08 min^{-1} (e). The errors in the determination of these rates, as determined from three to four repetitions of each experiment, were about 10% (see Table 3).

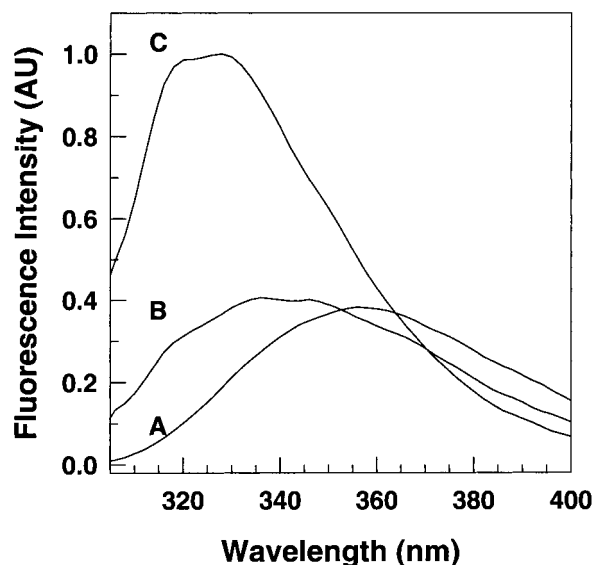


Figure 4. Fluorescence spectra of W38FW44F at 10°C in 8 M urea (a), during the first minute of the refolding process in 2 M urea (b), at equilibrium in 2 M urea (c). Excitation wavelength was 295 nm.

Time-resolved fluorescence measurements

To extract information about the local motion of Trp53 in the intermediate, the fluorescence lifetime of Trp53 was monitored at various time points after initiating the refolding reaction. Table 1 shows that the fluorescence decays could be fitted to a sum of three exponentials for the unfolded protein (in 8 M urea) and as a sum of two exponentials for the folded protein (in 2 M urea and also in the absence of urea). Three lifetimes have been observed for a large number of single tryptophan proteins in their unfolded form (Swaminathan *et al.*, 1994a, and references cited therein). The three lifetimes presumably arise from the three rotameric states of the tryptophan, all of which are expected to be populated in the unfolded state.

The evolution of the mean lifetime $\tau_m (= \sum \alpha_i \tau_i)$ with time of folding is shown in Figure 3(f). The apparent rate constant of the slow phase of folding, measured by the rate of change of τ_m , is 0.16 min^{-1} . This value is about two times faster than the rate of the slow phase observed in steady-state measurements including fluorescence intensity (Figure 3(a), (c)). Mean lifetime is normally proportional to steady-state fluorescence intensity (but

Table 1. Fluorescence lifetimes of W53 as a function of folding time

Time ^a (minutes)	Fluorescence lifetimes ^b (ns)			Amplitudes			Mean lifetime ^c (ns)	
	τ_1	τ_2	τ_3	α_1	α_2	α_3	τ_m	χ^2
0.0	5.52	1.74	0.16	0.32	0.27	0.41	2.29	1.2
0.7	5.00	1.63	0.21	0.63	0.20	0.17	3.45	1.0
1.4	5.00	1.80	0.21	0.65	0.20	0.15	3.62	1.1
2.0	5.02	1.65	0.21	0.63	0.21	0.16	3.56	1.1
2.8	4.96	1.65	0.21	0.67	0.18	0.15	3.65	1.2
3.6	5.05	1.75	0.21	0.68	0.19	0.13	3.80	1.0
4.5	5.00	1.70	0.21	0.71	0.19	0.10	3.88	1.1
5.1	5.05	1.75	0.21	0.73	0.18	0.09	4.03	1.0
5.9	4.97	1.65	0.21	0.75	0.18	0.07	4.04	1.1
6.7	5.01	1.66	0.21	0.76	0.18	0.05	4.17	1.0
7.5	4.98	1.51		0.81	0.19		4.31	1.0
8.4	5.02	1.60		0.80	0.20		4.32	0.9
9.3	4.95	1.63		0.84	0.16		4.40	1.1
10.1	4.98	1.55		0.82	0.18		4.38	0.9
11.0	4.94	1.50		0.84	0.16		4.41	1.0
12.3	4.94	1.50		0.84	0.16		4.39	1.1
13.2	4.96	1.40		0.85	0.15		4.43	0.9
14.0	4.95	1.50		0.85	0.15		4.44	1.1
15.8	4.98	1.50		0.85	0.15		4.45	0.9
16.7	4.91	1.40		0.86	0.14		4.40	0.9
18.7	4.94	1.41		0.86	0.14		4.43	0.9
20.8	5.00	1.48		0.84	0.16		4.45	1.1
23.1	4.99	1.68		0.85	0.15		4.49	1.0
26.6	5.00	1.62		0.85	0.15		4.50	0.9
30.8	5.00	1.60		0.85	0.15		4.48	1.0
44.4	4.95	1.50		0.88	0.12		4.51	1.0
56.2	4.99	1.68		0.85	0.15		4.50	1.0
60.9 ^d	4.93	1.40		0.88	0.12		4.49	1.1

^a Time after dilution of protein from 8 M to 2 M urea. Zero time corresponds to protein in 8 M urea before dilution.

^b The errors in the parameters are ~10%.

^c $\tau_m = \sum \alpha_i \tau_i$, $\sum \alpha_i = 1$.

^d The values of the parameters obtained at the last time point for folding in 2 M urea are identical to the values obtained for the protein in the absence of any urea.

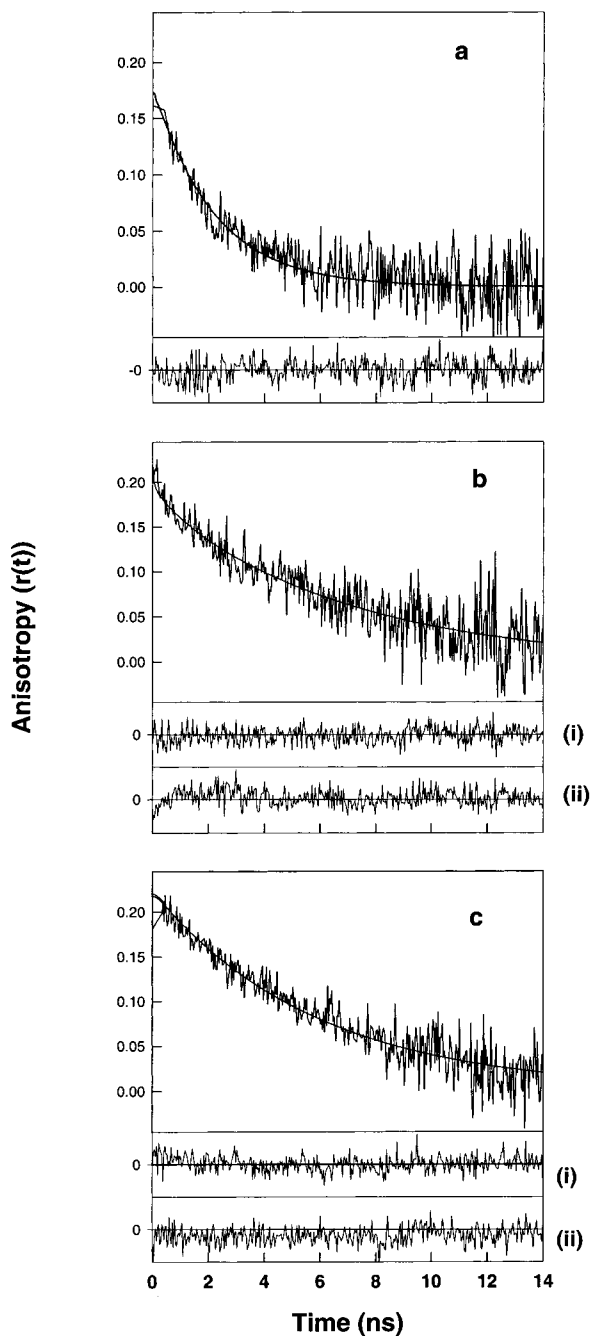


Figure 5. Decay of fluorescence anisotropy of W38FW44F at 10°C. (a) In 8 M urea. The lower panel shows the residuals for a single exponential fit with $\tau_r = 2.2$ ns. (b) During the first minute of the refolding process in 2 M urea. (i) Shows the residuals for a two exponential fit which gives $\tau_{r1} = 7.2$ ns and $\tau_{r2} = 1$ ns; (ii) Shows the residuals for a single exponential fit which gives a single $\tau_r = 6.2$ ns. (c) 56 minutes after the initiation of the refolding process (this decay is identical to that of the native protein), (i) shows the residual distribution for a single exponential fit with $\tau_r = 5.6$ ns, (ii) shows the residual distribution for a fit where τ_r was fixed around 7.2 ± 0.2 ns.

see below) because it represents the area under the intensity *versus* time of decay curve. Hence, mean

lifetime can be used to track the folding process (Eftink, 1994). The disagreement between the apparent rate constants associated with the slow phases of change in τ_m and fluorescence intensity would indicate the presence of either a very short lifetime component (as in static quenching) or a very long component, both outside our measurement range. Consequently, the results suggest that: (i) the level of static quenching of fluorescence of Trp53 changes as the protein molecules fold to N; and (ii) at least one additional intermediate state accumulates between that formed initially in the first minute, and the native protein at the completion of folding. The latter inference gets support from the time dependence of the shortest lifetime component (τ_3 in Table 1) which vanishes significantly faster than the time dependence of fluorescence intensity.

Information about rotational reorientation motions is better obtained from characterization of the time-resolved fluorescence anisotropy of Trp53 (Jacob *et al.*, 1997; Swaminathan *et al.*, 1994b, 1996; Lakshmikanth & Krishnamoorthy, 1999; Bilsel *et al.*, 1999). The anisotropy decay curves obtained for the native protein and the protein in 2 M urea are superimposable and could be analyzed as a single exponential with a rotational correlation time (τ_r) of 5.6 ns (Figure 5(c)). The agreement of this value with that of 5.7 ns calculated from NMR relaxation data of [^{15}N]nuclei of the barstar backbone (Sahu *et al.*, 2000; Wong *et al.*, 1997) is excellent. Also, this value agrees with that calculated for a protein of molecular mass 10,100 at 10°C (Cantor & Schimmel, 1980).

The decay of fluorescence anisotropy for the protein in 8 M urea is described by a single exponential with a τ_r of 2.2 ns. This is similar to our earlier observation (Swaminathan *et al.*, 1996). Anisotropy decay curves were determined at different times of refolding. The first decay curve obtained after initiation of refolding (~ 45 seconds) resembles that of the fully folded state more than that of the unfolded protein (Figure 5). Unlike the decay for the fully folded protein (Figure 5(c)), which was described well by a single exponential, the first decay at 45 seconds had, however, to be analyzed as a sum of two exponentials, with rotational correlation times ~ 7.2 ns and ~ 1.0 ns, because the residuals for a single exponential analysis clearly indicated a misfit (Figure 5(b), (i) and (ii)). The shorter correlation time (τ_{r2}) represents the internal mobility of Trp53 and the longer correlation time (τ_{r1}) corresponds to the global motion of the protein. A three-exponential analysis (with τ_r values ~ 7.2 ns, ~ 5.6 ns and ~ 1 ns, for example) did not improve either the χ^2 or the residuals of the fit. The decay could not, however, be fitted to a sum of only two exponentials with time constants of 5.6 ns and 0.5-1.5 ns. This indicates that the longer correlation time is significantly greater than 5.6 ns, which corresponds to the correlation time of the native protein. On the other hand, the residual distribution of the native protein when analyzed

with a τ_r of ~ 7.2 ns (Figure 5(c)(ii)) shows that the difference between 5.6 ns and 7.0 ns can be ascertained from the available data. As the folding progressed, the shorter τ_r (τ_{r2}) disappeared completely, well before the more gradual decrease of the longer τ_r (τ_{r1}) from 7.2 ns to 5.6 ns and (Table 2, Figure 6(a)). Finally only a single τ_r corresponding to that of the native protein ($\tau_r = 5.6$ ns) remained. It is also significant to point out the absence of the 2.2 ns component (which corresponds to the U state) even at the first time slice of the refolding kinetics. The kinetics of decrease of τ_{r1} were fit to equation (4) to obtain an apparent rate of 0.05 min^{-1} for the change in the average global rotational correlation time from 7.2 ns to 5.6 ns, which occurs as the protein folds (Figure 6(a)).

The fractional amplitude associated with τ_{r2} was 0.15 in the first time slice after commencement of folding. As folding progressed, this vanished to zero with an apparent rate constant of $0.24(\pm 0.06) \text{ min}^{-1}$ (Figure 6(b)). This rate, which represents the rigidification of the core of the protein, is significantly faster than either the kinetics of fluorescence intensity change (Figure 3(c)) or the kinetics of decrease of τ_{r1} (Figure 6(a)), but is similar to the kinetics of mean lifetime τ_m (Figure 3(f)). Results similar to the above were obtained when the protein concentration was increased by about fourfold. The possibility that a value of τ_r larger than 5.6 ns (corresponding to the N state) could be

due to the presence of aggregates is ruled out as such species are concentration dependent, and τ_r would then be expected to be larger at higher protein concentrations.

The steady-state anisotropy calculated from the time-resolved parameters (Swaminathan *et al.*, 1996) is given in Table 2. It may be noted that these r_{ss} values show the same change on initiation of refolding and remain nearly constant throughout the process, as was seen with the r_{ss} directly measured in the steady-state experiment (Figure 3(d)). The parameters given in Tables 1 and 2 are those obtained from a single kinetic run. Similar parameters were obtained in at least four independent kinetic runs.

Discussion

Accumulation of a late folding intermediate

Earlier studies had shown that in concentrations of denaturant equivalent to those used in this study, the folding of barstar proceeds through two pathways:

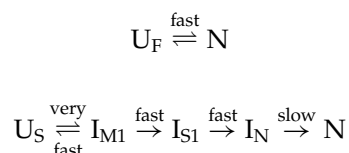


Table 2. Fluorescence anisotropy decay parameters as a function of time of folding

Time ^a (minutes)	Rotational correlation times ^b		Amplitudes		Initial anisotropy r_o	Steady state anisotropy ^c	
	τ_{r1}	τ_{r2}	β_1	β_2		r_{ss}	χ^2
0.0	2.20		1.00		0.20	0.08	1.1
0.7	7.29	1.00	0.85	0.15	0.22	0.12	1.0
1.6	7.00	1.15	0.87	0.13	0.22	0.12	1.0
2.4	6.72	1.00	0.91	0.09	0.21	0.12	1.0
4.2	6.75	1.00	0.92	0.08	0.21	0.12	0.9
5.0	6.73	1.00	0.91	0.09	0.21	0.12	0.9
5.8	6.95	1.00	0.94	0.06	0.21	0.12	0.9
6.7	6.84	1.03	0.95	0.05	0.21	0.12	0.9
7.6	6.90	1.00	0.96	0.04	0.21	0.12	1.0
8.5	6.76		1.00		0.21	0.12	1.0
9.3	6.48		1.00		0.21	0.11	1.0
10.2	6.45		1.00		0.21	0.12	1.1
11.5	6.58		1.00		0.21	0.12	1.0
13.6	6.39		1.00		0.21	0.12	1.0
15.9	6.23		1.00		0.22	0.11	0.9
20.1	6.05		1.00		0.21	0.12	1.0
23.0	5.90		1.00		0.21	0.12	1.0
25.5	5.82		1.00		0.21	0.12	1.1
28.1	5.61		1.00		0.22	0.12	1.0
31.7	5.57		1.00		0.21	0.12	1.0
34.6	5.71		1.00		0.21	0.12	0.9
37.2	5.55		1.00		0.21	0.12	1.0
41.6	5.59		1.00		0.21	0.12	0.9
45.1	5.60		1.00		0.21	0.12	1.1
52.8	5.69		1.00		0.22	0.12	1.0
60.4 ^d	5.58		1.00		0.21	0.12	1.1

^a Time after dilution of protein from 8 M to 2 M urea. Zero time corresponds to protein in 8 M urea before dilution.

^b The errors in the parameters are $\sim 20\%$ for τ_{r2} and $\sim 10\%$ for others.

^c r_{ss} was calculated from parameters given in Tables 1 and 2.

^d The values of the parameters obtained at the last time point for folding in 2 M urea are identical to the values obtained for the protein in the absence of any urea.

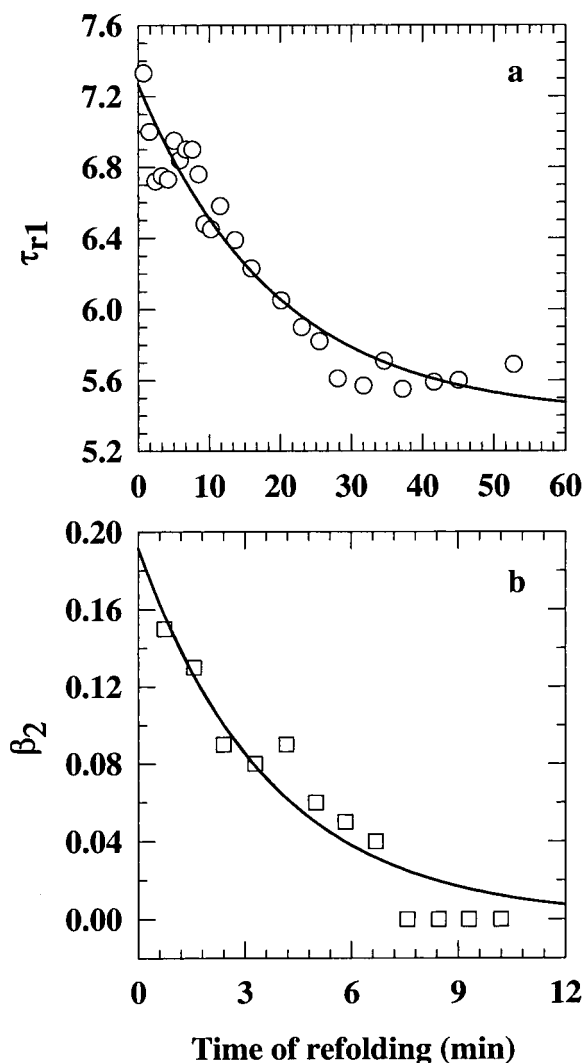


Figure 6. Kinetics of the long rotational correlation time (a) and the amplitude of the short correlation time (b) during the slow phase of refolding in 2 M urea. The continuous line in (a) is a fit to equation (4), while that in (b) is a fit to equation (3); they yield apparent rate constants $k_2 = 0.05(\pm 0.001) \text{ min}^{-1}$ (a) and $k_1 = 0.24(\pm 0.06) \text{ min}^{-1}$ (b), where the errors in the rates represent the standard deviations from four repetitions of the experiment.

U_F and U_S are two unfolded forms: U_F folds fast to native protein, while U_S folds more slowly. (Schreiber & Fersht, 1993; Shastry *et al.*, 1994). U_F folds to N with a time constant of less than 200 ms. U_S collapses to a compact state I_{M1} within 5 ms (Agashe *et al.*, 1995; Shastry & Udgaonkar, 1995). I_{M1} transforms to I_N in a biphasic process that involves at least one intermediate, I_{S1} : far-UV CD indicates that the $I_{M1} \rightarrow I_{S1}$ reaction occurs with a time constant of 50 ms, while near-UV CD indicates that the $I_{S1} \rightarrow I_N$ reaction has a time constant of 200 ms (Agashe *et al.*, 1995).

The data in Figure 2 suggest that after folding in 2 M urea at 10 °C has proceeded for ten seconds, which corresponds to the dead time of measurement in this study, 33(±4)% of the protein molecules have already folded to N, or to a form that has the same fluorescent properties as N, and which unfolds at the same rate as N. Earlier studies (Schreiber & Fersht, 1993; Shastry *et al.*, 1994; Shastry & Udgaonkar, 1995) had shown that equilibrium-unfolded protein at 25 °C consists of ~30% U_F and 70% U_S . The data in Figure 2 suggest that a change in temperature to 10 °C does not affect significantly the relative amounts of U_F and U_S . This result with barstar is similar to that seen in the case of ribonuclease A, where the equilibrium between U_F and U_S also appears to be independent of temperature (Schmid, 1982).

The product of the fast phase of folding of barstar has always been assumed to be native protein (Schreiber & Fersht, 1993; Shastry *et al.*, 1994) because it unfolds at the same rate as N, and its fluorescence is the same as that of N. Only 16% of the near-UV ellipticity of the native protein is however, recovered in the fast phase (Figure 3), whereas at least 33% should have been, if 33% of the molecules fold to N in the fast phase. This surprising result suggests that the product of the fast phase may not be N but is instead a very native-like state that unfolds at the same rate as N, but which possesses only half the final near-UV ellipticity of N.

After ten seconds of folding, the remaining ~67% of the molecules that started off as U_S have transformed to I_N (Schreiber & Fersht, 1993; Shastry *et al.*, 1994; Shastry & Udgaonkar, 1995). I_N possesses 20% of the native-state secondary structure, and only marginal tertiary structure (Figure 3). Furthermore, the fluorescence spectrum (Figure 4) as well as the mean lifetime of Trp53 in I_N suggests that it contains a hydrated and loosely packed mobile interior. Measurements of the rotational correlation time show that it increases from a value of 2.2 ns in the unfolded state to a value of 7.2 ns in I_N (Table 2). For the unfolded polypeptide, the value of 2.2 ns for the rotational correlation time at 10 °C compares well with the value of 1.5 ns reported in a previous study (Swaminathan *et al.*, 1996) at 25 °C. The observation that the rotational correlation time increases to 7.2 ns within the dead-time of measurement (Table 2) suggests that a high degree of chain compaction occurs during the formation of I_N . Even though it is a late folding intermediate, I_N appears to retain the properties expected for the product of a non-specific polypeptide collapse which experiences substantial rotational friction.

Structure of I_N

Spectroscopic properties of I_N can be estimated by extrapolating to $t = 0$ the kinetic curves determined by different optical probes, and subtracting out the contribution of the 33% molecules that

have already folded to N, whose optical properties are, of course, known. Thus, in 2 M urea I_N would appear to possess only 5% of the fluorescence intensity, 20% of the ellipticity at 222 nm and 100% of the fluorescence anisotropy characteristic of N.

I_N and N have been reported to differ in the (*trans versus cis*) isomeric state of the Y47-P48 bond (Schreiber & Fersht, 1993; Killick *et al.*, 1999). For barstar as well as for other proteins in which late intermediates, which differ similarly from the native protein in possessing X-Pro bonds in non-native isomeric states have been shown to accumulate, it has always been assumed that differences in structure between I_N and N are restricted to near the non-native bond (Schmid, 1992). The transition from I_N to N is therefore expected to involve only local structural arrangements. Thus, it was not surprising when it was shown that in the case of barstar, I_N appeared to be sufficiently native like and that it was capable of binding to and inhibiting barnase (Schreiber & Fersht, 1993). It must, however, be remembered that peptide fragments of barstar with no significant structure are able to bind to and inhibit barnase activity (Soler-Gonzalez & Fersht, 1997).

Here it is shown that several of the properties of I_N are incompatible with it being very native like. Far-UV CD measurements suggest that the secondary structure content of I_N is only 20% that of N, and near-UV CD measurements suggest that specific tertiary structures in the vicinities of the aromatic residues are absent. The fluorescence properties of I_N suggest that it lacks a well-defined protein core. In the native state, the side-chain of Trp53 is sequestered from the solvent and is lodged in the hydrophobic interior. The red-shifted fluorescence spectrum of I_N compared to that of N, as well as the low quantum yield of the tryptophan side-chain in I_N (5% of that in N), suggests that the core is largely accessible to the solvent. This is consistent with the ability of I_N to bind ANS (Figure 3(e)), which shows that certain hydrophobic groups are not configured to consolidate the core, but instead are solvent exposed. The global correlation time of 7.2 ns for I_N compared with 5.6 ns for N, provides further evidence that I_N and N are structurally very different. This view is consistent with recent ^1H NMR results (Bhuyan & Udgaonkar, 1999), which show a low degree of chemical shift dispersion of aromatic and aliphatic side-chain resonances in I_N .

Motional properties of Trp53 in I_N

The fluorescence of Trp53 is seen to decay in three exponential phases (Table 1), at the first time of observation after commencement of refolding. Three fluorescence lifetimes have also been observed for the protein under moderate to strongly denaturing conditions (Swaminathan *et al.*, 1996). Multi-exponential decay of tryptophan fluorescence in proteins has been suggested to originate

from multiple microstates or multiple structures of the protein (Harris & Hudson, 1990; Chabbert *et al.*, 1992; Kim *et al.*, 1993; Swaminathan *et al.*, 1994a). Accordingly, the environment of Trp53 in I_N must be poorly packed and highly mobile, so that the indole side-chain exists in multiple orientations around the C^α - C^β bond. In the native state of barstar, Trp53 is sandwiched by helix 1 and β -strand 2 (Lubienski *et al.*, 1994); thus, the indole side-chain is rigid, and a single rotamer appears to be populated preferentially, as the 4.9 ns lifetime component accounts for 88% of the amplitude of decay. It is, however, difficult to determine which rotamer is present in the native state in the absence of very high-resolution X-ray data.

Time-resolved fluorescence anisotropy reflects, directly, the mobility of the probe, and hence its hydrodynamic size and shape (Cantor & Schimmel, 1980; Gryczynski *et al.*, 1991). In the case of proteins, the observed dynamics generally comprise two components: (1) the motional freedom of the probe (tryptophan) with respect to the protein; and (2) global motion of the entire protein. The former has information on the internal flexibility and compactness around the probe and the latter could give an idea of the overall size and shape. Here, the anisotropy decay of Trp53 contains information on both these aspects. Firstly, a rotational correlation time (τ_r) of 7.2 ns observed at the first time of measurement indicates the formation of a compact structure. It also indicates that the hydrodynamic radius of the structure is slightly larger than that of the final N state ($\tau_r \sim 5.6$ ns). A value for τ_r of 7.2 ns could indicate either a globular form with hydrodynamic radius larger than that of the N state or a non-spherical (prolate) structural form (Fleming, 1985). If a spherical shape is assumed for I_N , the value of τ_r (7.2 ns) suggests that the volume of I_N exceeds that of N by $\sim 25\%$. This larger volume identifies I_N as a molten globule (Ptitsyn, 1992), consistent with its low secondary structure content and lack of specific tertiary interactions. The fluorescence spectrum and the low quantum yield of Trp53 in I_N indicates that water has not yet been extruded from the core, and suggests that I_N is a wet molten globule (Ptitsyn, 1992). Secondly, the observation of the short correlation time of ~ 1 ns during the early phase of the slow folding process indicates that the core is flexible in I_N . Thus, I_N is characterized by the presence of two types (*viz.*) (i) local and (ii) global) of motional freedom of W53.

The observation of a shorter correlation time of ~ 1 ns for I_N compared to 2.2 ns for the U form could be due to one or more of the following factors: (i) the U form is measured in 8 M urea, whose viscosity is 16% higher than that of 2 M urea used for measuring other species including I_N ; (ii) hindrance to local mobility is expected to be less in the compact I_N when compared to U, similar to observations in Subtilisin Carlsberg (Lakshmikanth & Krishnamoorthy, 1999); (iii) the 2.2 ns correlation time in U may be a combination

of the hindered side-chain motion and segmental motion.

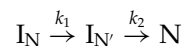
Dynamical evolution of I_N to the native form

The observable slow phase of barstar folding, which represents the $I_N \rightarrow N$ transition, has been monitored by several optical probes in this study (Table 3). Far-UV CD, near-UV CD, intrinsic tryptophan fluorescence and ANS fluorescence measurements indicate an apparent rate of $0.07(\pm 0.01) \text{ min}^{-1}$ for this process. Double-jump experiments suggest that native protein forms at a rate of $0.03(\pm 0.005) \text{ min}^{-1}$. The rotational correlation time corresponding to global motion changes with a rate of $0.05(\pm 0.01) \text{ min}^{-1}$. This range in rates is small, but significantly large compared to the errors in the individual measurements, and therefore points to the multi-state nature of the slow-folding reaction of barstar. In fact, a more detailed, recent study of the slow folding reaction of barstar (Bhuyan & Udgaonkar, 1999) has suggested that the small differences in rates measured using different steady-state optical probes as well as NMR probes are significant and real.

The evolution of rotational correlation times of Trp53 during the slow phase provides a picture of the changes in global motions required for folding of I_N . The longer correlation time, τ_{r1} , decreases at an apparent rate of 0.05 min^{-1} , slightly slower than the rate of formation of secondary and tertiary structures. These results suggest that the formation of secondary and tertiary structures is either concomitant with, or precedes, the final compaction of the polypeptide chain to its native state dimensions.

The time course of rigidification or consolidation of the hydrophobic core has been measured as the rate of disappearance of the amplitude of the faster, 1 ns rotational correlation time, τ_{r2} , to be $0.24(\pm 0.06) \text{ min}^{-1}$. This rate is significantly faster than the observed rates for secondary or tertiary

structure formation, final compaction of the polypeptide chain and formation of N, which fall in the range $0.03\text{-}0.08 \text{ min}^{-1}$. Thus, the $I_N \rightarrow N$ transition does not occur in one step, but in at least two distinct steps, and can be denoted, minimally, as:



Consolidation of the core occurs in the $I_N \rightarrow I_{N'}$ step, and the core residue Trp53, which is completely buried in N, becomes rigid in $I_{N'}$. This step is characterized by the disappearance of the faster correlation time (Figure 6(b)). $I_{N'}$ and N have a rigid core, and hence do not display the faster local motion of Trp53 seen in I_N . Since Trp53 maintains close hydrophobic contacts with seven other core residues in N, it is very likely that the entire hydrophobic core becomes rigid in this step. While I_N possesses only a small fraction (20%) of the secondary structure present in N, and virtually no tertiary interactions, the secondary and tertiary structural content of $I_{N'}$ can only be estimated (see below). Once the core becomes rigid in $I_{N'}$, formation of substantial secondary and tertiary structures follows during the $I_{N'} \rightarrow N$ reaction. At the same time, final compaction of the protein occurs, accompanied by water extrusion, and disappearance of water-exposed hydrophobic patches, leading to the formation of N.

Since the slow folding reaction of I_N to N observed here is 1000-fold slower than the faster folding reactions preceding it (Shastry & Udgaonkar, 1995), and because it is being studied under conditions in which all molecules fold to N; it can be considered independently of the fast folding reactions. The $I_N \rightarrow I_{N'} \rightarrow N$ mechanism dictates that there be a lag in the formation of N as the concentration of $I_{N'}$ builds up to its maximum value. Detection of the lag phase by the steady-state spectroscopic probes depends on the values of k_1 and k_2 , as well as on the spectroscopic properties of $I_{N'}$ relative to I_N and N. The data in Figures 2, 3 and 6 can be quantitatively fitted to

Table 3. Kinetics of the slow folding reaction of barstar

Probe	Rate (min^{-1}) ^a	Transition monitored ^b
1 Formation of N (double-jump experiment)	0.03 ± 0.005	$I_{N'} \rightarrow N$
2 Far-UV CD at 222 nm	0.07 ± 0.01	$I_N \rightarrow N$
3 Near-UV CD at 270 nm	0.08 ± 0.01	$I_{N'} \rightarrow N$
4 Steady state fluorescence of tryptophan at 330 nm	0.08 ± 0.01	$I_N \rightarrow N$
5 ANS fluorescence at 480 nm	0.08 ± 0.01	$I_N \rightarrow N$
6 Long rotational correlation time (representing average global motion)	0.05 ± 0.01	$I_N \rightarrow N$
7 Mean fluorescence lifetime of tryptophan	0.16 ± 0.02	$I_N \rightarrow I_{N'}$
8 Amplitude of short rotational correlation time (representing local motion around tryptophan)	0.24 ± 0.06	$I_N \rightarrow I_{N'}$

^a The errors given are standard deviations from the rates obtained from multiple repetitions of the kinetic experiments.

^b The kinetics monitored by probes 1 to 6 were fit to $I_N \rightarrow I_{N'} \rightarrow N$ mechanism (equation (4)), using $k_1 = 0.24 \text{ min}^{-1}$, as described in the text.

the $I_N \rightarrow I_{N'} \rightarrow N$ mechanism, and the values of k_1 and k_2 , as well as the spectroscopic properties of $I_{N'}$ can thereby be determined.

For the $I_N \rightarrow I_{N'} \rightarrow N$ mechanism, the changes in steady-state spectroscopic signal intensity, $S(t)$, and the change in the degree of consolidation of the core (as measured by the change in amplitude of the faster rotational correlation time (τ_{r2})), $C(t)$ are given by:

$$S(t) = S_{I_N} \times I_N(t) + S_{I_{N'}} \times I_{N'}(t) + S_N \times N(t) \quad (1)$$

$$C(t) = C_{I_N} \times I_N(t) + C_{I_{N'}} \times I_{N'}(t) + C_N \times N(t) \quad (2)$$

where S_i refers to the steady-state spectroscopic signal intensity corresponding to one mole of species i , C_i refers to the degree of consolidation of the core of one mole of species i , and $I(t)$ represents the concentration of species i at time t of folding.

The observed change in the degree of consolidation of the core is assumed to occur in the $I_N \rightarrow I_{N'}$ transition so that $C_{I_N} = 0$ and $C_{I_{N'}} = C_N = 1$. This assumption can be tested because the expressions for $I_N(t)$ and $N(t)$ are well known (Szabo, 1969; Shastry & Udgaonkar, 1995) for a $I_N \rightarrow I_{N'} \rightarrow N$ mechanism, so that $C(t)$ in equation (2) is given simply by:

$$C(t) = I_{N'}(t) + N(t) = A_0 e^{-k_1 t} \quad (3)$$

Thus, the disappearance of the amplitude of τ_{r2} is expected to follow single-exponential kinetics. The data in Figure 6(b) are, in fact, satisfactorily described by a single exponential process with an apparent rate, k_1 , of $0.24(\pm 0.06) \text{ min}^{-1}$.

The $I_N \rightarrow I_{N'} \rightarrow N$ mechanism must, of course, account also for the observed changes in intensities of steady-state spectroscopic signals (fluorescence, far-UV CD, near-UV CD). If the slow folding reaction is normalized to between 0 and 1, then $S_{I_N} = 0$ and $S_N = 1$. Thus, $S(t)$ (equation 1) is given by:

$$S(t) = S_{I_{N'}} I_{N'}(t) + N(t) \\ = \frac{(S_{I_{N'}} k_1 - A_0 k_2) e^{-k_1 t} + (A_0 - S_{I_{N'}}) k_1 e^{-k_2 t}}{k_2 - k_1} \quad (4)$$

The values of $S_{I_{N'}}$ and k_2 can be determined by fitting the data in Figure 3(a)-(c) to equation (4), using the value of k_1 (0.24 min^{-1}) by fitting the data in Figure 6(b) to equation (3). The slow folding data in Figure 3 fit well to equation (4), and yield values of 0.3 for $S_{I_{N'}}$ and $0.07(\pm 0.01) \text{ min}^{-1}$ for k_2 , from the time courses of change of steady-state signal intensities in Figure 3(a)-(c). No initial lag phase in the change of any steady-state spectroscopic signal intensity is observed, because one third of the spectroscopic changes that occur in the $I_N \rightarrow N$ reaction occur in the first $I_N \rightarrow I_{N'}$ step ($S_{I_{N'}} = 0.3$). In a kinetic simulation using equation (4) with $S_{I_{N'}}$ assumed to be zero, a small lag phase is indeed seen as expected, but only in the first 100 seconds.

The kinetics of formation of N (Figure 2), as measured by the double-jump experiments, were also fitted to equation (4) with $S_{I_{N'}}$ set to 0, because only molecules unfolding with the same rate as N are observed in these experiments. Again, according to equation (4), which describes the formation of N for a $I_N \rightarrow I_{N'} \rightarrow N$ mechanism, a lag in the formation of N should be seen in the first 100 seconds of refolding (see above). While the data fit well to equation (4), the goodness of fit is no different from that seen for a single exponential fit (Figure 2), given the $\leq 12\%$ error in the determination of N at each time point using the double jump assay. Thus, given the scatter in the data and the values of the observed rate constants, the data in Figure 2 are not good enough to distinguish between a $I_N \rightarrow I_{N'} \rightarrow N$ mechanism and a $I_N \rightarrow N$ mechanism.

It should also be noted that a lag phase would also not be observed if the transition from I_N to N occurs through the transient accumulation of not just one additional intermediate $I_{N'}$ but through a continuum of progressively more structured intermediates whose optical properties and size progressively approach that of N. The data in Table 3, showing a possible difference in rates of secondary and tertiary structure formation ($0.07(\pm 0.01) \text{ min}^{-1}$), final compaction ($0.05(\pm 0.01) \text{ min}^{-1}$) and formation of N ($0.03(\pm 0.005) \text{ min}^{-1}$) are not inconsistent with such a scenario.

An alternate model for explaining the slow phase (Figure 3) could be that the fast unobservable phase does not lead to complete transformation of U to $I_{N'}$, but instead an equilibrium is established between U and I_N before further transformation of $I_{N'}$. Then, the observable slow phase would represent not necessarily changes happening in the $I_N \rightarrow N$ step, but instead represent changes occurring during the preceding $U \rightarrow I_N$ step, to which it is kinetically coupled (Bhuyan & Udgaonkar, 1999). Such a model is, however, unlikely because no U state (characterized by τ_r value of 2.2 ns) can be detected, even at the first time point of our observation of the slow phase of folding in 2 M urea, 10°C . The time-evolution of steady-state anisotropy (Figure 3(d)) also indicates the absence of significant levels of U even during the initial part of the slow folding process. It should be pointed out that even if this alternative model were correct, the differences in rates of folding measured using different optical probes (Figures 3 and 6) would still lead to the same conclusions about when secondary and tertiary structure formation occur with respect to consolidation of the hydrophobic core.

Consolidation of the hydrophobic core during folding

The packing of amino acid residues in the hydrophobic core of a protein has a profound effect on stability and structure (Alber & Matthews, 1987; Axe *et al.*, 1996; Bashford *et al.*, 1987; Daopin *et al.*,

1991; Gassner *et al.*, 1996; Lim & Sauer, 1989, 1991; Munson & Regan, 1996; Reidhaar-Olson & Sauer, 1988). Hydrophobic core positions in a protein are most sensitive to mutations (Bashford *et al.*, 1987; Daopin *et al.*, 1991; Lim & Sauer, 1989, 1991; Reidhaar-Olson & Sauer, 1988), and the location of a destabilizing mutation is correlated with the rigidity of the position, as measured by crystallographic B factors (Alber & Matthews, 1987). The hydrophobic core appears to be packed in a unique and tightly constrained conformation (Ponder & Richards, 1987), and under-packing or over-packing of the core by mutagenesis leads to proteins that are either unstable or incorrectly folded. In cases where the hydrophobic core appears to be tolerant to drastic mutagenesis (Axe *et al.*, 1996; Gassner *et al.*, 1996), the mutant proteins retain very well-packed hydrophobic cores. Nevertheless, the observation that preferred interactions between hydrophobic side-chains are not seen in an analysis of known protein structures led to the suggestion that although tight packing is indispensable for the native conformation, it is not the causal agent for the native conformation (Behe *et al.*, 1991). In this study of the slow folding of barstar, it has been possible for the first time to relate the important process of the hydrophobic core becoming rigid to other structural events like compaction of the polypeptide chain, formation of secondary structure and formation of specific tertiary interactions.

Materials and Methods

Details of protein over-expression in the MM294 strain of *Escherichia coli* using the plasmid pMT316 encoding the barstar gene, and the procedure for protein purification have been described (Swaminathan *et al.*, 1996). Buffer solutions contained 20 mM sodium phosphate (pH 7), 300 μ M EDTA, and 250 μ M DTT. DTT was added ~one hour before measurements. Concentrations of urea in solutions were determined by refractive index measurements using an Abbe type refractometer (Milton Roy). All experiments were performed at 10 °C. A temperature of 10 °C was chosen to slow down the folding process in order to make time-resolved fluorescence measurements with sufficient signal-to-noise ratio (see below). A constant stream of nitrogen was blown on the outer surface of cuvettes and flow cells to prevent vapor condensation.

Steady-state measurement and analysis

For equilibrium unfolding measurements by fluorescence, barstar solutions (3 μ M) containing different concentrations of urea were incubated for ~12 hours. Tryptophan fluorescence excited at 295 nm was monitored at 10 °C at 330 nm. A photon-counting instrument (SPEX Fluorolog FL1T11) was used for the measurements. After correcting for associated buffer background signals, the raw equilibrium data were converted to a plot of f_N , the fraction of protein in the native state, versus the denaturant (D) using the following equation:

$$f_N = \frac{S_0 - [S_u + m_u[D]]}{[S_N + m_N[D]] - [S_u + m_u[D]]} \quad (5a)$$

where S_0 is the observed signal, S_f and S_u , and m_f and m_u represent intercepts and slopes of native and unfolded baselines estimated by linear extrapolation, respectively. The f_N plot was fitted to:

$$f_N = \frac{1}{1 + \exp\left[\frac{-\Delta G + m_G[D]}{RT}\right]} \quad (5b)$$

where ΔG corresponds to the free energy difference between the folded and unfolded states in the absence of any denaturant and m_G is a measure of cooperativity of the unfolding reaction. Also, $\Delta G = C_m m_G$, where C_m is the concentration of the denaturant at the midpoint of the transition.

For kinetic measurements, folding reactions were initiated by manual mixing of the required solutions. The dead time of measurement was ~ten seconds. The unfolded protein solutions, prepared in 8 M urea-containing buffer were incubated overnight. Folding was initiated by diluting one part of the unfolded protein into three parts of the refolding buffer containing no urea. The final protein concentrations in the refolding medium were ~4 μ M, ~60 μ M, and ~37.5 μ M for fluorescence, far-UV CD, and near-UV CD measurements, respectively. The signal of the native and of the unfolded protein of matching concentration was noted to facilitate normalization of the data. Following recording of kinetics, refractive indices of the solutions were read to calculate the concentration of urea in the refolding medium. Kinetics were recorded for ~two hours. Typically two to five traces were averaged. The data were fitted according to equation (4).

Ellipticity measurements were performed on a JASCO J720 instrument using a path length of 1 mm at 222 nm, and 1 cm at 270 nm.

Steady-state anisotropy was measured by monitoring the emission at parallel and perpendicular polarizations simultaneously by the use of the T-format optical arrangement of the SPEX fluorimeter. Experimentally obtained steady-state anisotropy data were compared to data simulated from the steady state intensities by assuming a two-state ($N \rightleftharpoons U$) model, using the following equations (Swaminathan *et al.*, 1996):

$$I_{ss} = \alpha_N \varepsilon_N \phi_N + \alpha_U \varepsilon_U \phi_U \quad (6)$$

$$r_{ss} = f_N r_N + f_U r_U \quad (7)$$

$$f_N = \alpha_N \varepsilon_N \phi_N / (\alpha_N \varepsilon_N \phi_N + \alpha_U \varepsilon_U \phi_U) \quad (8)$$

with

$$\alpha_N + \alpha_U = f_N + f_U = 1 \quad (9)$$

α_N and α_U are the mole fractions, and f_N and f_U are the fractions of the emitted photons corresponding to the N and U states, respectively. ε and ϕ are the molar extinction coefficient and the quantum yield, respectively. r_N and r_U are the anisotropy values corresponding to the N and U states, respectively. The fluorescence intensity data (Figure 3(c)) were fitted to equation (6) in order to get $\varepsilon_N \phi_N$, $\varepsilon_U \phi_U$ and the value of α_N at every time point during the refolding process. These values were then used to simulate r_{ss} by using equations (6)-(9) and the

values of r_N and r_U obtained at 0 and 8 M urea, respectively.

Double-jump experiments

The relative amount of N at any time of folding between 30 and 9000 seconds was determined by double-jump experiments as described (Shastry *et al.*, 1994, Shastry & Udgaonkar, 1995). The protein was unfolded to equilibrium in 8 M urea at 10 °C for six hours. Equilibrium unfolded protein was diluted four-fold to a final urea concentration of 2.0 M. After various times (30 to 9000 seconds) of refolding, the protein solution was diluted once more to raise the urea concentration to 5.5 M, to initiate unfolding. The rate and amplitude of the kinetic phase observed in the unfolding reaction were monitored. The rate of unfolding ($0.13(\pm 0.01) \text{ s}^{-1}$) identified the observable unfolding reaction to be that of N, while the relative amplitude indicated the relative amount of N present at the time of initiation of the unfolding reaction. The relative amplitudes were compared to the amplitude observed when refolding in 2 M urea was allowed to proceed for 12,000 seconds, when N is the only form of the protein present.

Measurement and analysis of time-resolved fluorescence

As in steady-state kinetic recording, time-resolved measurements were performed after diluting the protein manually into the folding buffer, the dead time of measurement now being ~ 45 seconds. Fluorescence intensity and anisotropy decays were measured by employing a CW mode-locked frequency-doubled Nd-YAG laser-driven dye (Rhodamine 6G) laser which generates 4-10 ps pulses (Periasamy *et al.*, 1988). The protein was excited by using the second harmonic output (295 nm) of an angle-tuned KDP crystal. Fluorescence decay curves were obtained by using a time-correlated single-photon counting setup coupled to a microchannel plate photo multiplier (Model 2809U; Hamamatsu Corp). Fluorescence intensity decays were deconvoluted with the instrument response function and analyzed as a sum of exponentials:

$$I(t) = \sum \alpha_i \exp(-t/\tau_i) \quad i = 1 - 3 \quad (10)$$

where $I(t)$ is the fluorescence intensity collected at the magic angle (54°) at time t and α_i is the amplitude associated with the i th fluorescence lifetime such that $\sum \alpha_i = 1$.

In the time-resolved anisotropy measurements, the emission was collected through a single channel by keeping the polarizer either parallel (I_{\parallel}) or perpendicular (I_{\perp}) to the polarization of the excitation beam. The anisotropy was calculated as:

$$r(t) = (I_{\parallel}(t) - I_{\perp}(t)G)/(I_{\parallel}(t) + 2I_{\perp}(t)G) \quad (11)$$

The accuracy of the estimated anisotropy decay parameters depended significantly on the accuracy of the grating (G) factor of the emission monochromator. Hence, extreme care was taken to estimate the G-factor by using *N*-acetyl tryptophanamide dissolved in phosphate buffer. Details of the instrument, the measurement techniques, and data analysis procedures are given else-

where (Periasamy *et al.*, 1988, Swaminathan *et al.*, 1994a,b).

Time-resolved anisotropy decays were analyzed on the basis of the model:

$$I_{\parallel}(t) = 1/3I(t)[1 + 2r(t)] \quad (12)$$

$$I_{\perp}(t) = 1/3I(t)[1 - r(t)] \quad (13)$$

$$r(t) = r_0 \sum \beta_j \exp(-t/\tau_j) \quad j = 1 \text{ or } 2 \quad (14)$$

where I_{\parallel} and I_{\perp} are the emission intensities collected at polarizations parallel or perpendicular to the polarization of the excitation beam, r_0 is the initial anisotropy, and α_i (equation (10)) and β_j are the amplitudes associated with the i th fluorescence lifetime and j th rotational correlation time such that $\sum \alpha_i = \sum \beta_j = 1$. Prior to the analysis of the anisotropy decays according to equations (12)-(14), the total intensity decay ($I(t)$) was generated ($I(t) = I_{\parallel}(t) + I_{\perp}(t)$). The propagation of errors associated with addition of the two decays was properly taken into account in the resultant decay. $I(t)$ so generated was analyzed to obtain fluorescence lifetimes and amplitudes (τ_i and α_i), which agreed very well with those obtained from the data collected directly at the magic angle. These lifetimes and amplitudes were then fixed during the analysis of the anisotropy decay, $I_{\parallel}(t)$ and $I_{\perp}(t)$ using equations (12)-(14) in order to reduce the number of floating parameters during the fit. Since the analysis of anisotropy decay involves multi-parameter fitting with several unknowns, the values obtained from the analysis were employed to calculate the steady-state anisotropy (r_{ss}):

$$r_{ss} = \frac{r_i \sum_i \sum_j \alpha_i \beta_j \left(\frac{1}{\tau_i} + \frac{1}{\tau_j} \right)^{-1}}{\sum_i \alpha_i \tau_j} \quad (15)$$

This value was compared with the experimentally measured value of the steady-state anisotropy at the same excitation and emission wavelengths under identical conditions. Only the set of parameters that gave the computed steady-state anisotropy value close to the observed value was accepted.

For obtaining anisotropy decays during the slow folding, the emission polarizer was rotated between the parallel and perpendicular positions during a single kinetic run. The anisotropy decay at each time point was generated using equation (11). The anisotropy decay parameters obtained at each time slice (~ 40 -60 seconds) were independent of the sequence of data collection in the two orientations ($I_{\parallel}(t)$, $I_{\perp}(t)$ or $I_{\perp}(t)$, $I_{\parallel}(t)$). This is expected for a slow process ($t_{1/2} \geq 10$ minutes) being monitored. The anisotropy decay parameters obtained were similar in many independent kinetic runs.

The time of measurement of the optical signal was typically 100 minutes. To be sure that no photo-bleaching of the protein was occurring during the long time of measurement, which would otherwise affect the measured rates, the optical signals of native and unfolded (in 8 M urea) protein were separately measured for the same period of time and found not to vary during the time of measurement (data not shown). These control experiments were carried out for both steady state and time-resolved measurements.

Acknowledgments

This work was funded by the Tata Institute of Fundamental Research, the Department of Biotechnology, Government of India, and by the Wellcome Trust. J.B.U. is the recipient of a Swarnajayanti Fellowship from the Government of India.

References

- Agashe, V. R., Shastry, M. C. R. & Udgaonkar, J. B. (1995). Initial hydrophobic collapse in the folding of barstar. *Nature*, **377**, 754-757.
- Alber, T. & Matthews, B. W. (1987). Temperature-sensitive mutations of bacteriophage T4 lysozyme occur at sites with low mobility and low solvent accessibility in the folded protein. *Biochemistry*, **26**, 3754-3758.
- Axe, D. D., Foster, N. W. & Fersht, A. R. (1996). Active barnase variants with completely random hydrophobic cores. *Proc. Natl Acad. Sci. USA*, **93**, 5590-5594.
- Bashford, D., Chothia, C. & Lesk, A. M. (1987). Determinants of a protein fold. Unique features of the globin amino acid sequences. *J. Mol. Biol.* **196**, 199-216.
- Beechem, J. M. (1997). Picosecond fluorescence decay curves collected on millisecond time scale: direct measurement of hydrodynamic radii, local/global mobility, and intramolecular distances during protein-folding reactions. *Methods Enzymol.* **278**, 24-49.
- Behe, M. J., Lattman, E. E. & Rose, G. D. (1991). The protein-folding problem: the native fold determines packing, but does packing determine the native fold? *Proc. Natl Acad. Sci. USA*, **88**, 4195-4199.
- Bhuyan, A. K. & Udgaonkar, J. B. (1999). Observation of multistate kinetics during the slow folding and unfolding of barstar. *Biochemistry*, **38**, 9158-9168.
- Bilsel, O., Yang, L., Zitzewitz, J. A., Beechem, J. M. & Matthews, C. R. (1999). Time-resolved fluorescence anisotropy study of the folding reaction of the α -subunit of tryptophan synthase reveals non-monotonic behavior of the rotational correlation time. *Biochemistry*, **38**, 4177-4187.
- Cantor, C. R. & Schimmel, P. R. (1980). *Biophysical Chemistry*, W. H. Freeman & Co., New York.
- Chabbert, M., Hillen, W., Hansen, D., Takahashi, M. & Bousquet, J. A. (1992). Structural analysis of the operator binding domain of Tn10-encoded Tet repressor: a time-resolved fluorescence and anisotropy study. *Biochemistry*, **31**, 1951-1960.
- Chan, C. K., Hu, Y., Takahashi, S., Rousseau, D. L., Eaton, W. A. & Hofrichter, J. (1997). Submillisecond protein folding kinetics studied by ultrarapid mixing. *Proc. Natl Acad. Sci. USA*, **94**, 1779-1784.
- Chen, L., Wildegger, G., Kiefhaber, T., Hodgson, K. O. & Doniach, S. (1998). Kinetics of lysozyme refolding: structural characterization of a non-specifically collapsed state using time-resolved X-ray scattering. *J. Mol. Biol.* **276**, 225-237.
- Daopin, S., Alber, T., Baase, W. A., Wozniak, J. A. & Matthews, B. W. (1991). Structural and thermodynamic analysis of the packing of two alpha-helices in bacteriophage T4 lysozyme. *J. Mol. Biol.* **221**, 647-667.
- Dill, K. A., Bromberg, S., Yue, K., Fiebig, K. M., Yee, D. P., Thomas, P. D. & Chan, H. S. (1995). Principles of protein folding - a perspective from simple exact models. *Protein Sci.* **4**, 561-602.
- Eftink, M. R. (1994). The use of fluorescence methods to monitor unfolding transitions of proteins. *Biophys. J.* **66**, 482-501.
- Eliezer, D., Jennings, P. A., Wright, P. E., Doniach, S., Hodgson, K. O. & Tsuruta, H. (1995). The radius of gyration of an apomyoglobin folding intermediate. *Science*, **270**, 487-488.
- Fleming, G. R. (1985). *Chemical Applications of Ultrafast spectroscopy*, Oxford University Press Inc., New York.
- Gassner, N. C., Baase, W. A. & Matthews, B. W. (1996). A test of the "jigsaw puzzle" model for protein folding by multiple methionine substitutions within the core of T4 lysozyme. *Proc. Natl Acad. Sci. USA*, **93**, 12155-12158.
- Gast, K., Zirwer, D., Muller-Frohne, M. & Damaschun, G. (1998). Compactness of the kinetic molten globule of bovine alpha-lactalbumin: a dynamic light scattering study. *Protein Sci.* **7**, 2004-2011.
- Gryczynski, I., Steiner, R. F. & Lakowicz, J. R. (1991). Intensity and anisotropy decays of the tyrosine calmodulin proteolytic fragments, as studied by GHz frequency-domain fluorescence. *Biophys. Chem.* **39**, 69-78.
- Gutin, A. M., Abkevich, V. I. & Shakhnovich, E. (1995). Is burst hydrophobic collapse necessary for protein folding? *Biochemistry*, **34**, 3066-3076.
- Harris, D. L. & Hudson, B. S. (1990). Photophysics of tryptophan in bacteriophage T4 lysozymes. *Biochemistry*, **29**, 5276-5285.
- Jacob, M., Schindler, T., Balbach, J. & Schmid, F. X. (1997). Diffusion control in an elementary protein folding reaction. *Proc. Natl Acad. Sci. USA*, **94**, 5622-5627.
- Jones, B. E., Beechem, J. M. & Matthews, C. R. (1995). Local and global dynamics during the folding of *Escherichia coli* dihydrofolate reductase by time-resolved fluorescence spectroscopy. *Biochemistry*, **34**, 1867-1877.
- Killick, T. R., Freund, S. M. V. & Fersht, A. R. (1999). Real-time NMR studies on a transient folding intermediate of barstar. *Protein Sci.* **8**, 1286-1291.
- Kim, S. J., Chowdhury, F. N., Younathan, W. S. E. S., Rosso, P. S. & Barkley, M. D. (1993). Time-resolved fluorescence of the single tryptophan of *Bacillus stearothermophilus* phosphofructokinase. *Biophys. J.* **65**, 215-226.
- Kuwajima, K., Yamaya, H., Miwa, S., Sugai, S. & Nagamura, T. (1987). Rapid formation of secondary structure framework in protein folding studied by stopped-flow circular dichroism. *FEBS Letters*, **221**, 115-118.
- Ladurner, A. G. & Fersht, A. R. (1999). Upper limit of the time scale for diffusion and chain collapse in chymotrypsin inhibitor 2. *Nature Struct. Biol.* **6**, 28-31.
- Lakshmikanth, G. S. & Krishnamoorthy, G. (1999). Solvent-exposed tryptophans probe the dynamics at protein surfaces. *Biophys. J.* **77**, 1100-1106.
- Lim, W. A. & Sauer, R. T. (1989). Alternative packing arrangements in the hydrophobic core of lambda repressor. *Nature*, **339**, 31-36.
- Lim, W. A. & Sauer, R. T. (1991). The role of internal packing interactions in determining the structure and stability of a protein. *J. Mol. Biol.* **219**, 359-376.
- Lubienski, M. J., Bycroft, M., Freund, S. M. & Fersht, A. R. (1994). Three-dimensional solution structure

- and ¹³C assignments of barstar using nuclear magnetic resonance spectroscopy. *Biochemistry*, **33**, 8866-8877.
- Matouschek, A., Kellis, J. T., Jr, Serrano, L., Bycroft, M. & Fersht, A. R. (1990). Transient folding intermediates characterized by protein engineering. *Nature*, **46**, 440-445.
- Munson, M. & Regan, L. (1996). What makes a protein a protein? Hydrophobic core designs that specify stability and structural properties. *Protein Sci.* **5**, 1584-1593.
- Munson, M., Anderson, K. S. & Regan, L. (1997). Speeding up protein folding: mutations that increase the rate at which Rop folds and unfolds by over four orders of magnitude. *Folding Des.* **2**, 77-87.
- Nath, U., Agashe, V. R. & Udgaonkar, J. B. (1996). Initial loss of secondary structure in the unfolding of barstar. *Nature Struct. Biol.* **3**, 920-923.
- Nölting, B., Golbik, R. & Fersht, A. R. (1995). Submillisecond events in protein folding. *Proc. Natl Acad. Sci. USA*, **92**, 10668-10672.
- Nölting, B., Golbik, R., Niera, J. L., Soler-Gonzalez, A. S., Schreiber, G. & Fersht, A. R. (1997). The folding pathway of a protein at high resolution from microseconds to seconds. *Proc. Natl Acad. Sci. USA*, **94**, 826-830.
- Nymeyer, H., Garcia, A. E. & Onuchic, J. N. (1998). Folding funnels and frustration in off-lattice minimalist protein landscapes. *Proc. Natl Acad. Sci. USA*, **95**, 5921-5928.
- Panick, G., Malessa, R., Winter, R., Rapp, G., Frye, K. J. & Royer, C. A. (1998). Structural characterization of the pressure-denatured state and unfolding/refolding kinetics of staphylococcal nuclease by synchrotron small-angle X-ray scattering and Fourier-transform infrared spectroscopy. *J. Mol. Biol.* **275**, 389-402.
- Periasamy, N., Doraiswamy, S., Maiya, G. B. & Venkataraman, B. (1988). Diffusion controlled reactions: fluorescence quenching of cationic dyes by charged quenchers. *J. Chem. Phys.* **88**, 1638-1651.
- Plaxco, K. W. & Baker, D. (1998). Limited internal friction in the rate-limiting step of a two-state protein folding reaction. *Proc. Natl Acad. Sci. USA*, **95**, 13591-13596.
- Plaxco, K. W., Millet, I. S., Segel, D. J., Doniach, S. & Baker, D. (1999). Chain collapse can occur concomitantly with the rate-limiting step in protein folding. *Nature Struct. Biol.* **6**, 554-556.
- Ponder, J. W. & Richards, F. (1987). Tertiary templates for proteins. Use of packing criteria in the enumeration of allowed sequences for different structural classes. *J. Mol. Biol.* **193**, 775-791.
- Ptitsyn, O. B. (1992). The molten globule state. In *Protein Folding* (Creighton, T. E., ed.), pp. 243-300, W. H. Freeman & Co., New York.
- Reidhaar-Olson, J. F. & Sauer, R. T. (1988). Combinatorial cassette mutagenesis as a probe of the informational content of protein sequences, **241**, 53-57.
- Roder, H. & Colon, W. (1997). Kinetic role of early intermediates in protein folding. *Curr. Opin. Struct. Biol.* **7**, 15-28.
- Roder, H., Elove, G. & Englander, S. W. (1988). Structural characterization of folding intermediates in cytochrome c by H-exchange labelling and proton NMR. *Nature*, **335**, 700-704.
- Sahu, S. C., Bhuyan, A. K., Majumdar, A. & Udgaonkar, J. B. (2000). Backbone dynamics of Barstar: an ¹⁵N NMR relaxation study. *Proteins: Struct. Func. Genet.* In the press.
- Sali, A., Shakhnovich, E. & Karplus, M. (1994). How does a protein fold? *Nature*, **369**, 248-251.
- Schmid, F. X. (1982). Proline isomerization in unfolded ribonuclease A. The equilibrium between fast-folding and slow-folding species is independent of temperature. *Eur. J. Biochem.* **128**, 77-80.
- Schmid, F. X. (1992). Kinetics of unfolding and refolding of single-domain proteins. In *Protein Folding* (Creighton, T. E., ed.), pp. 197-241, W. H. Freeman & Co, New York.
- Schreiber, G. & Fersht, A. R. (1993). The refolding of *cis*- and *trans*-peptidyl prolyl isomers of barstar. *Biochemistry*, **32**, 11195-11203.
- Segel, D. J., Hofrichter, J., Hodgson, K. O., Doniach, S. & Kiefhaber, T. (1999). Characterization of transient intermediates in lysozyme folding with time-resolved small-angle X-ray scattering. *J. Mol. Biol.* **283**, 489-499.
- Semisotnov, G. V., Kihara, H., Kotova, N. V., Kimura, K., Amemiya, Y., Wakabayashi, K., Serdyuk, I. N., Timchenko, A. A., Chiba, K., Nikaido, K., Ikura, T. & Kuwajima, K. (1996). Protein globularization during folding. A study by synchrotron small-angle X-ray scattering. *J. Mol. Biol.* **262**, 559-574.
- Shastry, M. C. & Roder, H. (1998). A continuous-flow capillary mixing method to monitor reactions on the microsecond time scale. *Nature Struct. Biol.* **5**, 385-392.
- Shastry, M. C. & Udgaonkar, J. B. (1995). The folding mechanism of barstar: evidence for multiple pathways and multiple intermediates. *J. Mol. Biol.* **247**, 1013-1027.
- Shastry, M. C., Agashe, V. R. & Udgaonkar, J. B. (1994). Quantitative analysis of the kinetics of denaturation and renaturation of barstar in the folding transition zone. *Protein Sci.* **3**, 1409-1417.
- Soler-Gonzalez, A. S. & Fersht, A. R. (1997). Helix stability in barstar peptides. *Eur. J. Biochem.* **249**, 724-732.
- Sosnick, T., Shtilerman, M. D., Mayne, L. & Englander, S. W. (1997). Ultrafast signals in protein folding and the polypeptide contracted state. *Proc. Natl Acad. Sci. USA*, **94**, 8545-8550.
- Stryer, L. (1965). The interaction of a naphthalene dye with apomyoglobin and apohemoglobin. A fluorescent probe of non-polar binding sites. *J. Mol. Biol.* **13**, 482-495.
- Swaminathan, R., Krishnamoorthy, G. & Periasamy, N. (1994a). Similarity of fluorescence lifetime distributions for single tryptophan proteins in the random coil state. *Biophys. J.* **67**, 2013-2023.
- Swaminathan, R., Periasamy, N., Udgaonkar, J. B. & Krishnamoorthy, O. (1994b). Molten globule-like conformation of barstar: a study by fluorescence dynamics. *J. Phys. Chem.* **98**, 9270-9278.
- Swaminathan, R., Nath, U., Udgaonkar, J. B., Periasamy, N. & Krishnamoorthy, G. (1996). Motional dynamics of a buried tryptophan reveals the presence of partially structured forms during denaturation of barstar. *Biochemistry*, **35**, 9150-9157.
- Szabo, Z. G. (1969). Kinetic characterization of complex reaction systems. In *Comprehensive Chemical Kinetics* (Bamford, C. H. & Tipper, C. F. H., eds), vol. 2, pp. 1-80, Elsevier, New York.
- Thirumalai, D. (1995). From minimal models to real proteins - time scales for protein folding kinetics. *J. De Physique*, **5**, 1457-1467.

- Udgaonkar, J. B. & Baldwin, R. L. (1988). NMR evidence for an early framework intermediate on the folding pathway of ribonuclease A. *Nature*, **335**, 694-699.
- Waldburger, C. D., Jonsson, T. & Sauer, R. T. (1996). Barriers to protein folding: formation of buried polar interactions is a slow step in acquisition of structure. *Proc. Natl Acad. Sci. USA*, **93**, 2629-2634.
- Wong, K. B., Fersht, A. R. & Freund, S. M. (1997). NMR ^{15}N relaxation and structural studies reveal slow conformational exchange in barstar C40/82A. *J. Mol. Biol.* **268**, 494-511.
- Ybe, J. A. & Kahn, P. C. (1994). Slow-folding kinetics of ribonuclease-A by volume change and circular dichroism: evidence for two independent reactions. *Protein Sci.* **3**, 638-649.

Edited by C. R. Matthews

(Received 21 February 2000; received in revised form 5 July 2000; accepted 17 July 2000)